



# Improved inverse design method for thin-wall hollow profiled polymer extrusion die based on FEM-CFD simulations

Guangdong Zhang<sup>1,2</sup> · Xiang Huang<sup>1</sup> · Shuanggao Li<sup>1</sup> · Chao Xia<sup>3</sup> · Tong Deng<sup>4</sup>

Received: 30 July 2019 / Accepted: 3 December 2019 / Published online: 2 January 2020  
© Springer-Verlag London Ltd., part of Springer Nature 2020

## Abstract

Extrusion process has excellent capability in continuous manufactures with high production volume, low cost, and steady quality for very complex cross-sectional products. However, manufacturing a proper extrusion die is challenging, but essential for qualified products, which needs to consider many influence factors in the die design. This paper shows an improved inverse design method for thin-wall hollow profiled polymer extrusion die by using computational fluid dynamics simulation. Also, the design criteria of the inverse design method for extrusion die are proposed and discussed. The simulation results show that the thickness of the die lip gap can be enlarged with the decreasing of the inlet flow rate. Additionally, it shows that the geometry profile of the die lip gap can be widened with the increasing of the length of the free jet. The analytical results have been verified by experiments and show a good agreement. It is concluded that the improved inverse design method with FEM-CFD simulations can provide better accuracy and significantly reduce the manufacturing difficulty of micro and thin-walled extrusion die.

**Keywords** Inverse design · Design criteria · Profile extrusion dies · FEM-CFD · Polyflow

## 1 Introduction

Compared to other polymer processing technologies, polymer extrusion has many advantages and huge application prospects, which has been widely used in industry [1]. The main advantage of the polymer extrusion process is continuously manufactured uniform cross-sectional shapes with high production volume, low cost, and steady quality. With the above benefits, the polymer extrusion products have been widely applied in the field of construction, lighting, automobile,

medical, and so on. Generally, the extrusion process mainly includes raw material melting, forming, cooling and shaping, drawing, and cutting of the products. According to the types of the extrudate, there are different types of extrusion dies [1–3] such as pipe dies, sheet dies, spiral mandrel dies, and profile dies. One of the complex extrudates is the profile, such as automobile weatherstrip [4], tire components [5], and hollow profile [6].

A major problem in polymer extrusion process is die swell due to velocity profile rearrangement and recovery of the elastic deformation [7, 8]. The degree of die swell is usually described by die swell ratio, which is defined as  $R_S = S_{ex}/S_0$ , where  $S_{ex}$  is the cross-section area of the extrudate and  $S_0$  is the cross-section area of the extrusion die gap. The die swell ratio is mainly influenced by material properties, process conditions, and deformation history of the material in the extrusion die. Therefore, the design of a proper die is essential for quality of the products with correct dimension of the profile. In the past, lots of great efforts have been made by using a trial-and-error procedure, which needs enormous time and results in huge costs [9]. Recently, development of numerical analysis technology has significantly improved design efficiency of the sophisticated geometry profile extrusion die [10–12], which remarkably reduce the numbers of trials and the total production costs.

---

**Electronic supplementary material** The online version of this article (<https://doi.org/10.1007/s00170-019-04785-w>) contains supplementary material, which is available to authorized users.

---

✉ Guangdong Zhang  
gdzhang@nuaa.edu.cn

- <sup>1</sup> College of Mechanical and Electrical Engineering, Nanjing University of Aeronautics & Astronautics, Nanjing, China
- <sup>2</sup> School of Mechanical Engineering, Yancheng Institute of Technology, Yancheng, China
- <sup>3</sup> Shanghai Bethlehem Plastic Co. Ltd., Shanghai, China
- <sup>4</sup> The Wolfson Centre for Bulk Solids Handling Technology, Faculty of Engineering and Science, University of Greenwich, London, UK

Because of die swell, the outline of the extrudate is different from the die exit, which manifests as profile distortion. Nowadays, there are two conventional methods which can be used to deal with the die swell problem in the industry. The first method is to achieve a flow balance at the die exit by adjusting the die geometry [6, 13]. This method is an optimization process, which aims to maximize the flow uniformity at the die exit by geometric modification of the die contour [14–16]. Based on sectional areas divided, the flow balance method should strike a balance between the thicker sub-areas where they have a higher flow-speed and the thinner sub-areas where they have a lower flow-speed, and eventually to make the average velocity homogeneously in all sub-areas of the die lip.

The flow-balance method has been widely used. Pauli et al. [17] and Siegbert et al. [18, 19] adopted space-time finite element method to the optimization of die design, in which the flow balance and homogeneous die swell were used as the design objectives. Yilmaz et al. [20] took uniformity of velocity distribution at the die exit as an objective function. Carneiro et al. [21] proposed a method only by using OpenFOAM et al. open-source software to aid the design of complex extrusion dies. Mu et al. [6] analyzed the influence of the die geometric parameters on the velocity distribution uniformity. Rajkumar et al. [22] introduced a novel method to balance the flow distribution in complex extrusion dies, in which the profile cross-section geometry should be divided into L- and T-shaped profiles. However, the major drawback of the flow balance method is its computational domain that only includes the die domain, not the free jet domain. Therefore, the die-swell effect and consequent extrusion deformation are not taken into account.

The second method attempts to compensate for the effects of die swell, which is called inverse design method. Covas et al. [23] mentioned a strategy to correct the die lip by considering the die swell effect. Legat et al. [24] discussed the inverse extrusion problem (IEP), which was to find a required die shape through implicit Newton-Raphson iterative method. Gifford [25] suggested that the design of complex profile extrusion dies often involved not only “balancing” the die but also compensating for the effects of die swell. These efforts [26] show that this method can improve the design of profile extrusion dies for complex shapes, but the main difficulty is limited methodological guidance available, especially for the criteria of the inverse design for micro and thin-walled extrusion die.

In this paper, the inverse design method was used for finding an optimal solution of a thin-wall hollow profiled extrusion die by using computational fluid dynamics simulation. Based on the simulation results, criteria of the inverse design method of extrusion die were proposed and discussed. Experiment study was carried out, and the measured values of geometric dimensions of the extruded parts were obtained, which show a good agreement with the expectation.

## 2 Problems in design of extrusion die

In the design of an extrusion die, many difficulties occurred, which are mainly due to the die swell and consequent distortion in different areas when the material leaves the die. For thin-wall hollow profile, one major problem is the thickness control of the die lip gap where it is too thin to do the die repair. A typical example of thin-wall hollow profiles is shown in Fig. 1, which is investigated in the following study.

This profile is a transparent plastic light cover and installed in the aluminum strip profile. The hollow profile has almost a uniform wall thickness of 1.5 mm. From previous experiences, the required wall thickness of the profile is hard to be achieved and should be adjusted by the successive approximation of the die repair. If the wall thickness deviation is too big, it will increase the times of die repair and even causes die failures. Up to now, there is no effective method to solve this problem, neither the flow balance method nor the inverse design method.

### 2.1 CFD model for extrusion process

To solve the problem effectively, a CFD model is established based on the assumption that the polymer melts are incompressible laminar viscous non-Newtonian fluids flowing under isothermal conditions. Also, the effect of inertia and gravity has not been considered in the CFD simulation.

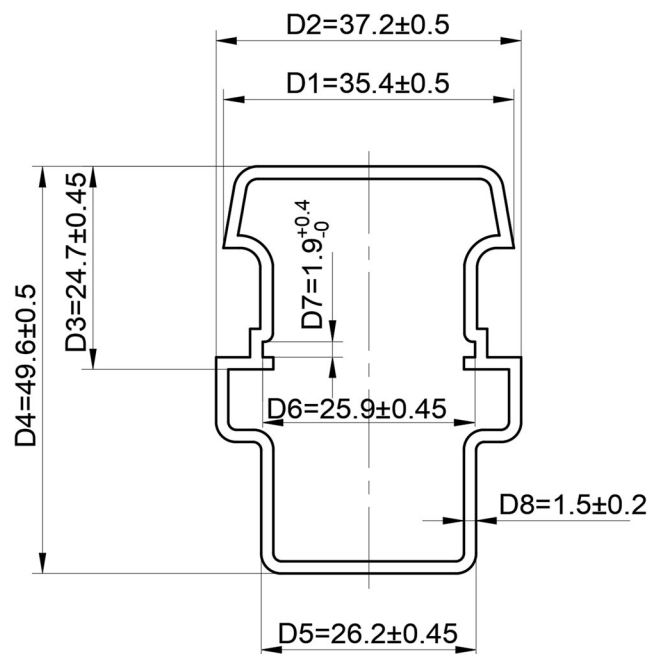


Fig. 1 Cross-sectional geometric parameters of a thin-wall hollow profile (dimension in mm)

## 2.2 Material properties

The product material showed in Fig. 1 is polycarbonate (Makrolon ET3113). Its melt temperature is 300 °C, and melt density is 1.02 g/cm<sup>3</sup>. Polycarbonate melts are high viscous non-Newtonian fluids so that elasticity can be neglected in numerical simulation. The shear viscosity  $\eta(\dot{\gamma})$  in Eq. 1 is a function of the second invariant of the rate of deformation tensor using the Bird-Carreau viscous model [27] for the shear-rate dependence of viscosity.

$$\eta(\dot{\gamma}) = \eta_{\infty} + \frac{\eta_0 - \eta_{\infty}}{\left(1 + (\lambda\dot{\gamma})^2\right)^{(1-n)/2}} \quad (1)$$

where  $\eta_{\infty}$  is infinite-shear viscosity (0 Pa·s),  $\eta_0$  is the zero-shear viscosity (707 Pa·s),  $\lambda$  is the relaxation time (0.00243 s), and  $n$  is the power-law index (0.426). The rheological parameters were obtained from Computer Aided Material Preselection by Uniform Standards (CAMPUS) database [28] and checked by using a rheometer (HAAKE RS600, Thermo Electron, USA) from East China University of Science and Technology.

## 2.3 Boundary conditions

Conventionally, flow runner of a profiled extrusion die often included the adapter, transition section, pre-parallel section, parallel section (die land), and the extrusion mandrel for hollow profile [29]. As mentioned by Dai et al. [30], if the length of the parallel section is long enough, the influence of the transition section and the pre-parallel section on the extrusion simulation can be neglected. So in this simulation, the parallel section (die land domain) and the free surface (free jet domain) were included in the computational domain (shown in Fig. 2). The length of die land domain and free jet domain are  $L_D$  and  $L_F$ , respectively. Due to the symmetry of the problem, a symmetry boundary condition is specified for the sake of simplicity. In die land

domain, the polymer melts enter the die from inlet and leave die lip, concurrently the no-slip boundary condition is applied at wall. The die lip is the interface between die land domain and free jet domain. After the polymer melt leaves the die lip, a die swell occurs and the polymer melts move toward the outlet of the free jet under a traction force. Finally, a free surface is formed after the polymer melts have been extruded.

The boundary conditions were specified in ANSYS Polyflow:

Boundary 1: Inlet. The fully developed velocity profile was computed by the ANSYS Polyflow and with the volumetric flow rate  $Q$  in mm<sup>3</sup>/s.

Boundary 2: Outlet, at which a constant drawing velocity or force was imposed.

Boundary 3: Plane of symmetry, which has the zero tangential force  $f_s = 0$ , and normal displacement  $d_n = 0$ .

Boundary 4: Free surface, where does the die swell happen. Arbitrary Lagrangian-Eulerian (ALE) interface-tracking method and Optimesh-3D remeshing method were used for simulating a free surface in ANSYS Polyflow.

Boundary 5: Wall with the no-slip boundary condition.

## 2.4 Mesh generation

The 3D model has been meshed with hexahedral elements using ANSYS Meshing module. Because of its symmetric property, only half of the geometry has been meshed (see Fig. 3).

The length of the die land is 60 mm and the free jet is 30 mm. The total number of nodes and elements are 215,840 and 185,325, respectively. Around the die lip area, the meshes have been refined to improve the mesh quality, because of large deformation around the die lip zone. From the results of mesh convergence study, the effect of grid

**Fig. 2** 3D geometry and boundary conditions in the simulation

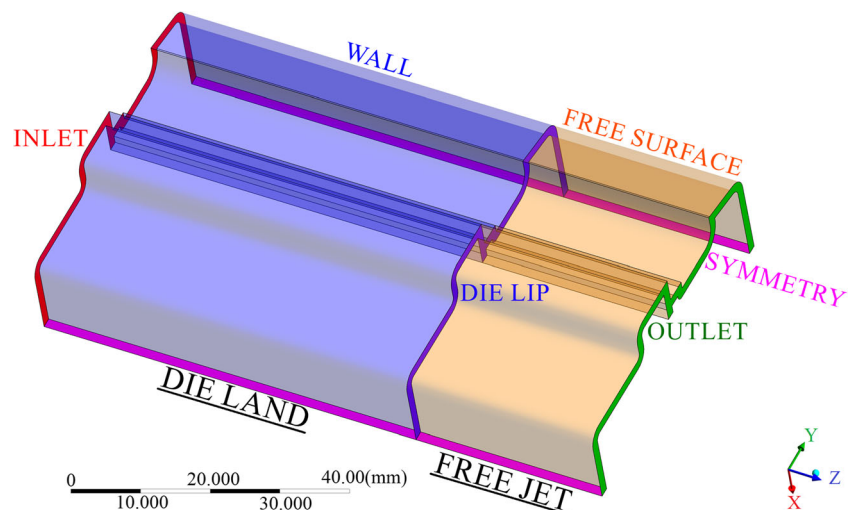
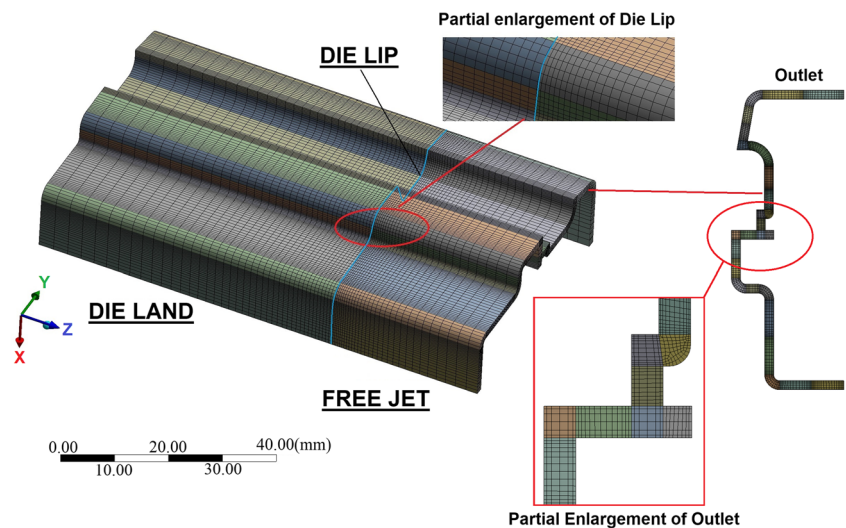


**Fig. 3** Mesh generation for the extrusion simulation



accuracy on the simulation results is within 0.3% if the number of nodes in the thickness direction is more than six.

## 2.5 CFD simulation results

### 2.5.1 Prediction of extrudate swell

In the design of an extrusion die, engineers need to know the deformation of the extrudate occurred, which is called prediction of extrudate swell [31, 32]. With CFD simulation using finite element software ANSYS Polyflow, the prediction of extrudate swell can be achieved. The boundary conditions are defined: the volumetric flow rate  $Q$  of the INLET is  $1321.1 \text{ mm}^3/\text{s}$  based on the product of the area of die lip gap and the expected extrusion velocity of  $10 \text{ mm/s}$ , and the outlet of the free jet has zero drawing force applied.

It can be found that the velocity distribution at the die exit is nearly balanced from the simulation results shown in Fig. 4. However, there is a high-velocity region at the middle of the die exit where the maximum velocity is  $18.25 \text{ mm/s}$ . Due to velocity redistribution out of the die exit, a local higher velocity results in a more significant extrusion distortion [1]. The average velocity at the die lip of the die land is reduced from  $8.27$  to  $7.95 \text{ mm/s}$  at the outlet of free jet. Meanwhile, the cross-sectional area is increased from  $132.018 \text{ mm}^2$  of the die lip to  $166.568 \text{ mm}^2$  of the extrudate, and thus, the die swell ratio ( $R_S = S_{ex}/S_0$ ) in this simulation is 1.262.

Because the thickness of the die lip is constant and the thickness of the extrudate is uniform except for the corner sections, the thickness at the middle of the six straight sections of the extrudate was used to obtain an average thickness (see Fig. 4). It is shown that the average thickness is increased from  $1.5 \text{ mm}$  at the die lip gap to  $1.813 \text{ mm}$  at the extrudate.

For the results, it shows that the extrusion deformation and thickness swell are unacceptable, and compensation is needed

for the profile extrusion die. Due to the complexity of the hollow profile, it is hard to get the right dimension of extrudate by the optimization method for flow balance.

## 2.6 Inverse design method

An inverse design method has been applied for finding a possible solution of the extrusion die design to produce the desired profile after the die swell happened. The cross-section of the extrudate is taken as input and the extrusion die lip as output in the inverse extrusion simulation. The boundary conditions are the same as the previous ones in Sect. 4.1. As the expected extrusion velocity of  $10 \text{ mm/s}$  and the expected area of outlet is  $132.11 \text{ mm}^2$ , the volumetric flow rate of the outlet is  $1321.1 \text{ mm}^3/\text{s}$ . By continuity equations for incompressible fluids, the volumetric flow rate from inlet to outlet is constant. Therefore, the volumetric flow rate  $Q$  of the inlet is  $1321.1 \text{ mm}^3/\text{s}$ . Due to the fact that application of drawing force may impact the simulation results, in this case, the outlet of the free jet has zero drawing force applied. Importantly, the inverse prediction should be activated in die land domain to implement the inverse design of extrusion die.

The profile of the die lip gap is similar to the required profile of the extrudate, as shown in Fig. 5. The simulation results show that the cross-sectional area of the die lip is  $105.187 \text{ mm}^2$ , compared with  $132.018 \text{ mm}^2$  of the extrudate, and therefore, the die swell ratio here is 1.255. Due to the effect of die swell, the average velocity was reduced from  $10.41 \text{ mm/s}$  at the die lip to  $9.99 \text{ mm/s}$  at the outlet of free jet. Meanwhile, the average thickness of the die lip gap is  $1.20 \text{ mm}$ , which leads to a difficulty in the manufacture of the extrusion die. Here, the thickness at the middle of the six straight sections of the die lip was used for calculating an average value.

Fig. 4 Six locations of the extrudate (left) and velocity distribution at the die lip and extrudate swell prediction (right)

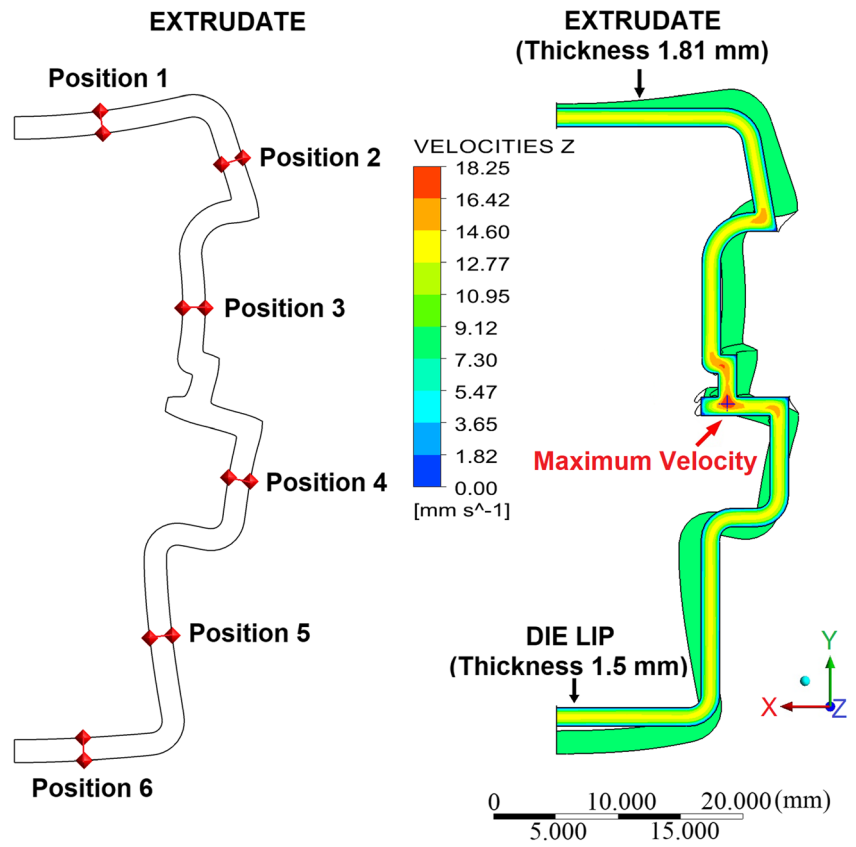
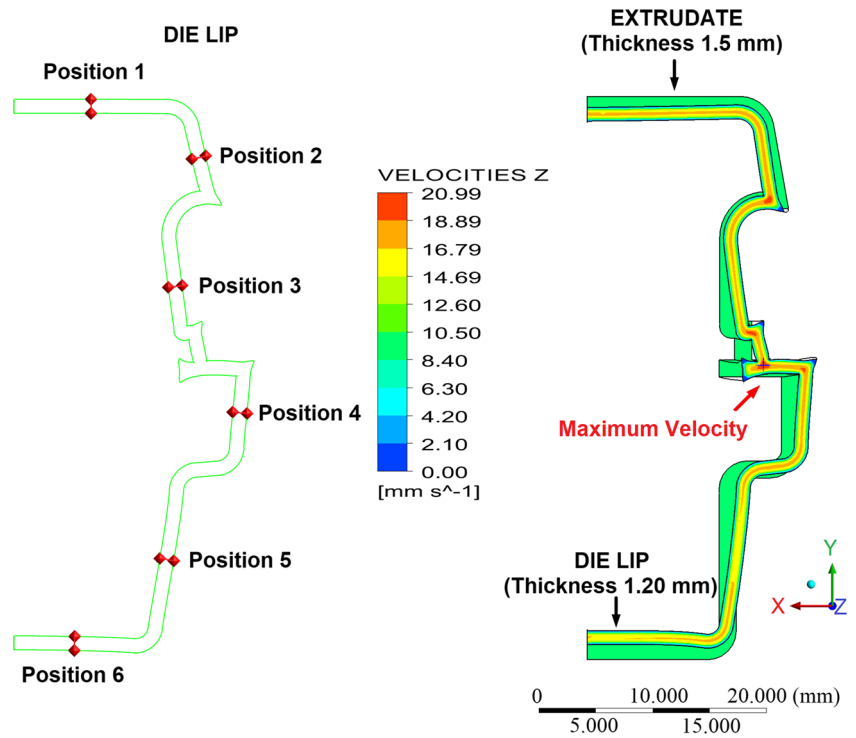


Fig. 5 Six locations of the die lip (left) and velocity distribution and profile geometry of the die lip by inverse design (right)



**Table 1** Variation of the thickness of die lip at different positions with inlet volumetric flow rate

Flow rate [mm <sup>3</sup> /s]	Average [mm]	Position 1 [mm]	Position 2 [mm]	Position 3 [mm]	Position 4 [mm]	Position 5 [mm]	Position 6 [mm]
1100	1.76	1.78	1.76	1.74	1.76	1.76	1.77
1150	1.66	1.67	1.66	1.64	1.66	1.66	1.67
1200	1.57	1.57	1.57	1.55	1.57	1.57	1.57
1250	1.48	1.49	1.49	1.47	1.49	1.48	1.49
1300	1.41	1.41	1.41	1.39	1.41	1.41	1.41
1350	1.34	1.34	1.35	1.32	1.35	1.34	1.34
1400	1.28	1.28	1.28	1.26	1.28	1.28	1.28

## 2.7 Improved inverse design method and design criteria

In simulation results shown in Fig. 5, the drawing velocity has not been considered. If the drawing velocity applied at the outlet is larger than 9.99 mm/s, the extrudate will shrink in the cross-section dimensions. Instead, if the drawing velocity remains constant, the reduction of the inlet volumetric flow rate  $Q$  will also result in the decrease of velocity at the die lip. Consequently, the extrudate will shrink too. Thus, the dimension of the die lip gap should be enlarged to compensate for the shrinkage. In the case, if the thickness of the die lip needs to increase, the volumetric flow rate of inlet should decrease or the drawing velocity should increase. As the increase of drawing velocity results in the subsequent difficulty of calibration and cooling, the approach of reducing the inlet volumetric flow rate is selected for the above purpose.

According to the above analysis, the relationship of inlet volumetric flow rate with the thickness of die lip at six different positions (shown in Fig. 5) is studied, as illustrated in Table 1. The volumetric flow rate  $Q$  of the inlet is changed from 1100 to 1400 mm<sup>3</sup>/s. Also, a constant drawing velocity (10 mm/s) has been applied at the outlet. For the simulation results, the thickness at different positions with the same flow rate condition is nearly uniform, so the average thickness of the die lip can be used for subsequent discussion. Also, the

results show that the average thickness of the die lip increases with the decrease of the inlet flow rate.

For convenience, thickness swell ratio and length swell ratio are defined in Eqs. 2 and 3:

$$R_{TS} = \frac{T_{ex}}{T_0} \quad (2)$$

where  $T_{ex}$  is the average thickness of extrudate and  $T_0$  is the average thickness of die lip.

$$R_{LS} = \frac{L_{ex}}{L_0} \quad (3)$$

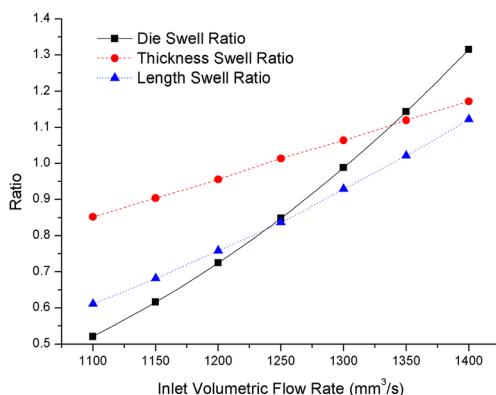
where  $L_{ex}$ ,  $L_0$  is the development length along the centerline of extrudate and die lip, respectively.

It is difficult to measure the development lengths along the centerline from the results. However, if small branches of the extrudate can be ignored, the area of extrudate is approximately equal to the thickness of extrudate times the development length along the centerline of extrudate ( $S_{ex} = L_{ex} \times T_{ex}$ ). In the same way, the area of die lip can be defined as  $S_0 = L_0 \times T_0$ . Thus, the length swell ratio can be formulated as

$$R_{LS} = \frac{L_{ex}}{L_0} = \frac{S_{ex}/T_{ex}}{S_0/T_0} = \frac{S_{ex}/S_0}{T_{ex}/T_0} = \frac{R_S}{R_{TS}} \quad (4)$$

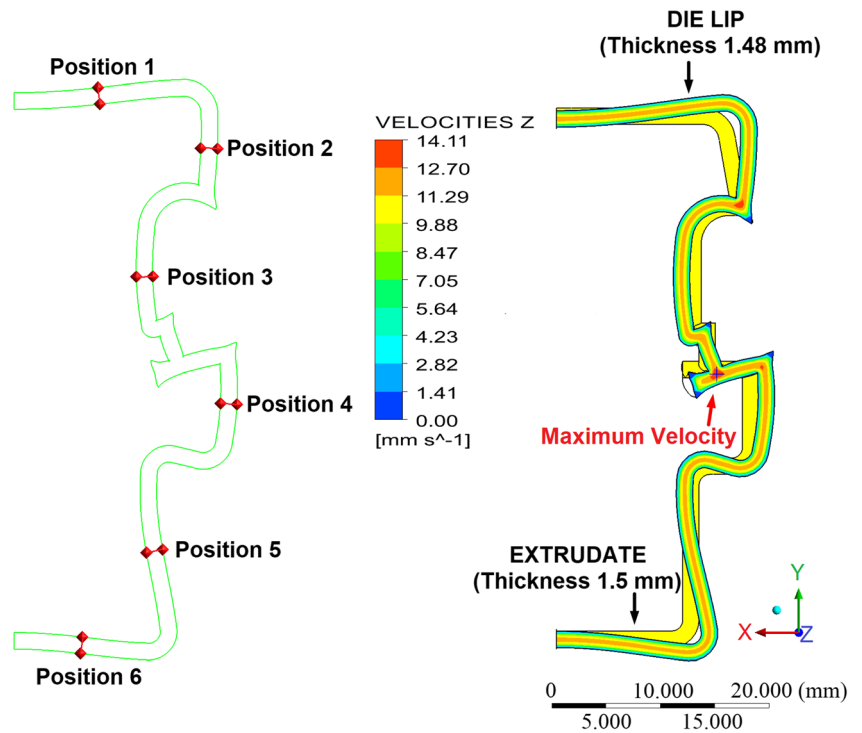
The relationship of die swell ratio ( $R_S = S_{ex}/S_0$ ), thickness swell ratio ( $R_{TS}$ ), and length swell ratio ( $R_{LS}$ ) with inlet volumetric flow rate has been studied, as shown in Fig. 6, which is useful for guidance of the profile extrusion die design and dimensional control of the extrudate.

Figure 6 indicates that, when the inlet flow rate increases from 1100 to 1400 mm<sup>3</sup>/s, the die swell ratio increases from 0.52 to 1.31, while the thickness swell ratio rises from 0.85 to 1.17, and the length swell ratio expands from 0.61 to 1.12, correspondingly. Compared with thickness swell ratio, the length swell ratio is smaller and more sensitive to the variation of inlet volumetric flow rate. In other words, in the inverse design of extrusion die, the variation ratio of development length along the centerline is bigger than the thickness of die lip, which can be found in Eqs. (2) and (3). As the increase in development length over a limited space means an increase in



**Fig. 6** Die swell ratio, thickness swell ratio, and length swell ratio with inlet volumetric flow rate

**Fig. 7** Six locations of the die lip (left) and velocity distribution and profile geometry of the enlarged die lip (right)



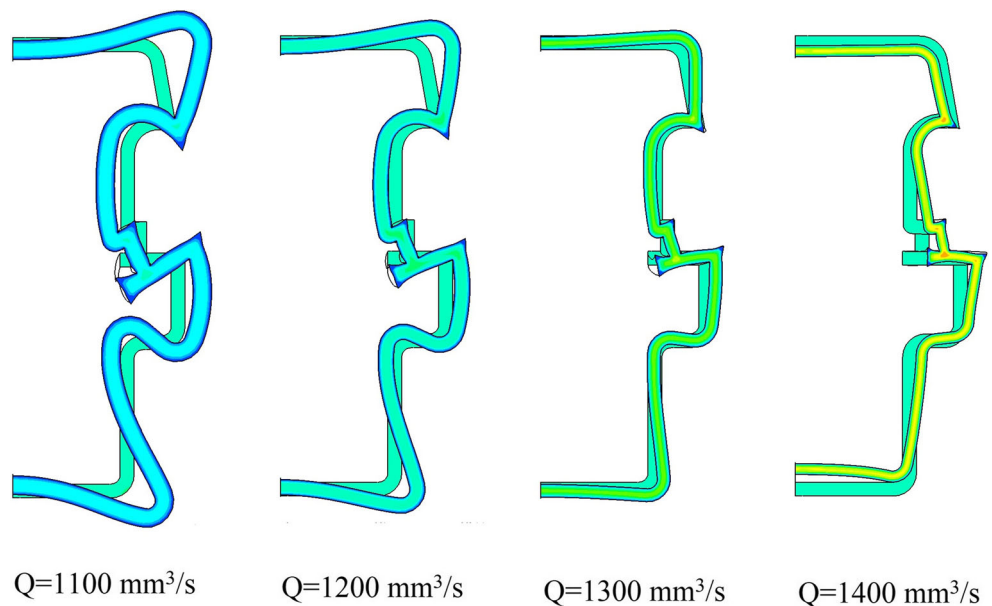
deformation, the length swell ratio can represent the degree of extrusion deformation.

Design criteria of improved inverse design of the extrusion die must be (1) maximum thickness of die lip and (2) minimum extrusion deformation. In other words, the thickness swell ratio should be minimized, and the length swell ratio needs to be close to one. However, the above criteria cannot be satisfied together, as shown in Fig. 7. Therefore, the design criterion needs to be that the thickness swell ratio is equal to one ( $R_{TS} = 1$ ), which means that the die swell ratio is equal to

the length swell ratio ( $R_S = R_{LS}$ ). The optimum solution of inlet flow rate can be found, which is equal to 1250 mm<sup>3</sup>/s.

The simulation results of the improved solution are shown in Fig. 7, where the die swell ratio is reduced to 0.848. The thickness of the die lip gap is 1.48 mm, compared with the 1.5 mm of the extrudate. The distortion of the die lip gap is acceptable, which is eligible for the manufacture of the extrusion die. By using this criterion and improving inverse design method, the manufacturing difficulty of the die is effectively reduced, and the extrusion deformation is within an acceptable

**Fig. 8** Die Lip gaps compared at different inlet volumetric flow rate Q



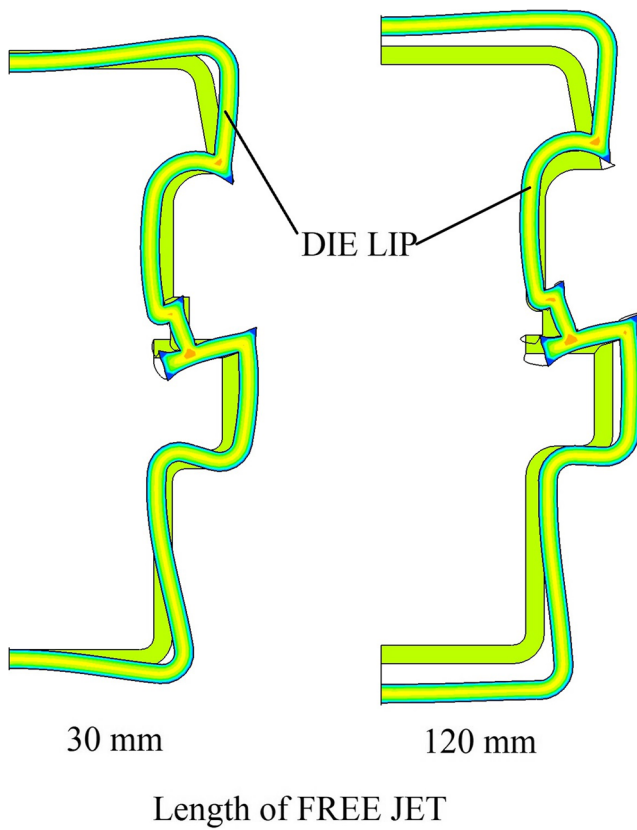


Fig. 9 Die lip gap compared (inlet volumetric flow rate  $Q = 1250 \text{ mm}^3/\text{s}$ )

range. This simulation results will be used for subsequent experimental verification.

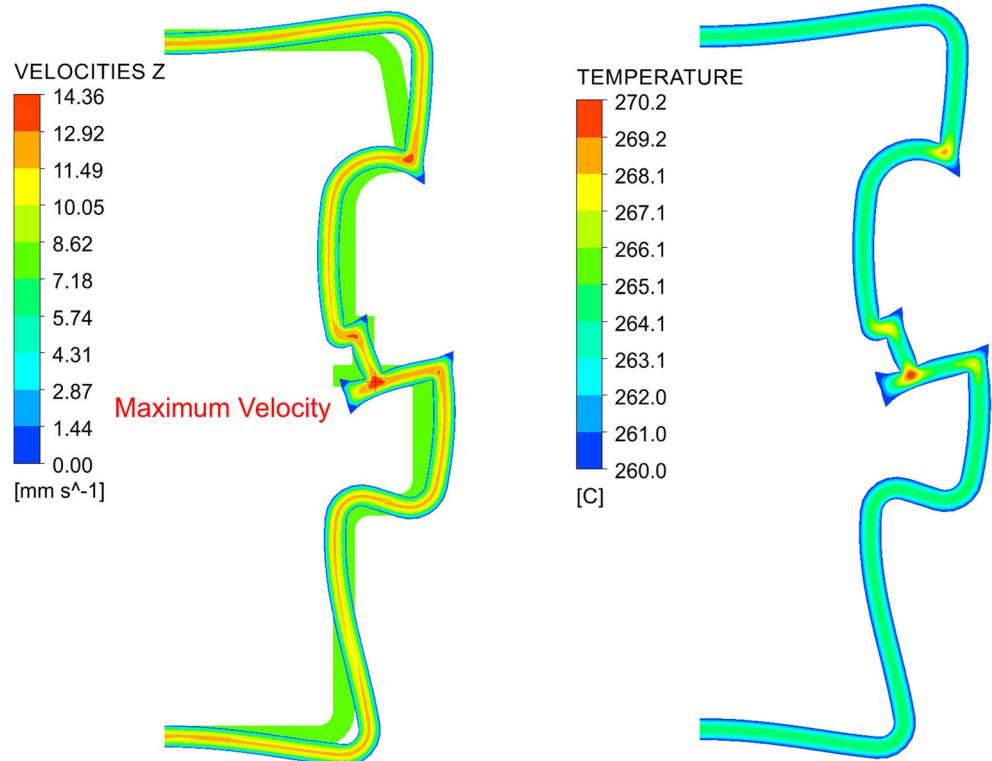
### 3 Discussion

With the decrease of the inlet flow rate, the distortion of the die lip gap will increase, as shown in Fig. 8. When the inlet volumetric flow rate  $Q$  is less than  $1100 \text{ mm}^3/\text{s}$ , the die lip gap will overlap itself at the center of the die lip, which is unacceptable in the design of extrusion die. The main reason is that the length swell ratio is quickly reduced as inlet flow rate decreased, and thus, the development length along the centreline of die lip will be elongated and twist itself in a limited space.

In the inverse design of extrusion die, the length of die land and free jet will also have a certain impact. As the length of the die land ( $L_D$ ) increases, the pressure drop in the profile extrusion die increases accordingly, as described previously [33]. When the length of free jet ( $L_F$ ) increased, the geometry profile of the die lip gap will be enlarged, but the thickness of the die lip will not change much as shown in Fig. 9. The increase in the length of the free surface also provides more spaces for adjusting the small-sized products.

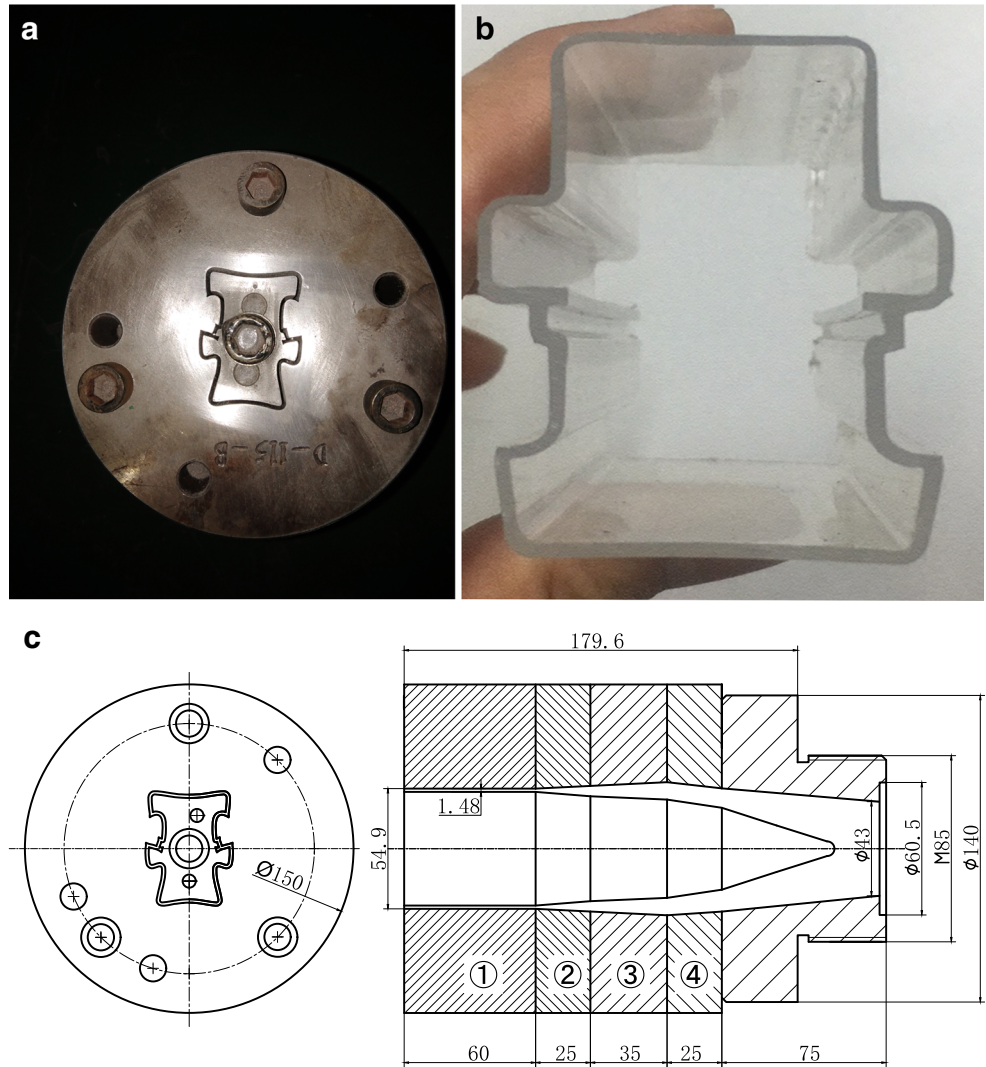
Although satisfactory results have been obtained by using isothermal fluid model and viscous material constitutive model, non-isothermal fluid model and viscoelastic material constitutive model are still necessary for the higher precision

Fig. 10 Velocity and temperature distribution of the enlarged die lip (non-isothermal)





**Fig. 11** Experiment results. **a** Experimental extrusion die. **b** Extrudate. **c** Drawing of extrusion die



extrusion, especially for viscoelastic materials with a low power-law coefficient. As a non-isothermal generalized Newtonian fluid, the apparent viscosity is related to the temperature in addition to the shear rate. The viscosity-temperature dependence is characterized by Arrhenius law:

$$H(T) = \exp \left[ \alpha \left( \frac{1}{T-T_0} - \frac{1}{T_\alpha-T_0} \right) \right] \tag{5}$$

where  $\alpha$  is the ratio of the activation energy ( $5.37 \times 10^3$  J) and  $T_\alpha$  is the reference temperature (300 °C),  $T_0$  is the absolutely zero temperature (− 273.15 °C). The inlet temperature of melts is 300 °C and the mold temperature is 260 °C. Specific heat capacity is 1.70 J/g-°C, thermal conductivity is 0.173 W/m-K, and coefficient of thermal expansion is 65.0  $\mu\text{m}/\text{m}^\circ\text{C}$ .

The results of a non-isothermal simulation are shown as in Fig. 10. The profile of the die lip obtained by non-

**Table 2** Target value and measured value of extruded parts

No.	Target value [mm]	Measurement (A) [mm]	Measurement (B) [mm]	Measurement (C) [mm]
D1	35.4±0.5	34.97	34.93	34.99
D2	37.2±0.5	36.99	36.91	36.93
D3	24.7±0.45	24.96	24.77	24.84
D4	49.6±0.5	49.98	49.93	50.01
D5	26.2±0.45	26.47	26.47	26.47
D6	25.9±0.45	25.85	26.10	25.77
D7	1.9+0.4/−0	1.98	2.06	2.05

isothermal simulation and isothermal simulation are similar. Meanwhile, the high-speed zone is also a high-temperature zone. The maximum temperature is 270 °C, which is bigger than the die temperature. It means that the choice of mold temperature is reasonable. Through non-isothermal simulation, we can get more accurate analysis results. Therefore, it is necessary to adopt non-isothermal simulation for the die with less space for adjustment.

### 3.1 Experimental evaluation

Extrusion experiment was implemented on the actual extrusion production line of Shanghai Bethlehem Plastic Co. Ltd. For the experimental study, a  $\Phi 65$ -mm single screw extruder machine (Maker: Jiangsu Faygo Union Machinery Co., Ltd.). The experimental extrusion die shown in Fig. 11a was manufactured according to the drawing of extrusion die shown in Fig. 11c, in which the profile of the enlarged die lip gap (shown in Fig. 7) is adopted. The experiment has the process parameters as follows. The inlet volumetric flow rate is 1250 mm<sup>3</sup>/s, and the drawing speed is 10 mm/s. The length of the die 1 to die 4 is 60 mm, 25 mm, 35 mm, and 25 mm, respectively. Meanwhile, the distance between die lip and calibrator is 30 mm.

The experimental results show a good product appearance and dimensional accuracy, which is shown in Fig. 11b. According to the experiment results, the extrusion die designed by the improved inverse method is qualified and cogent for the hollow profile extrusion. Because the overall profile of the extruded part is rectangular, the results are similar to the literature [1]. In the case of a square profile, the die exit required to attain a square profile is not square due to the influence of die swell, as illustrated by Kostic [1]. Therefore, the extrudate is regular, but the required die shape is irregular.

Three samples of extruded parts, named A, B, and C, were selected for measurement. The cross-sectional geometry and tolerance requirements of the product are shown in Fig. 1, and the target values are also listed in Table 2. It can be seen from the table that all dimensions are within the tolerance range. However, some dimensions such as D1 and D2 are close to the lower limit, and D4 is close to the upper limit, but the overall trend of the same dimension is basically the same.

The same three samples of extruded parts, named A, B, and C, were used to measure the thickness distribution of the part. The expected thickness of extruded parts is  $1.5 \pm 0.2$  mm. The positions of all measurement points are shown in Fig. 12.

It can be seen from Table 3 that all dimensions are within the tolerance range; some dimensions such as T5, T6, and T12 are close to the lower limit. The reason for the problem may be that the flow resistance in these areas is large and needs to be improved in the subsequent repair process.

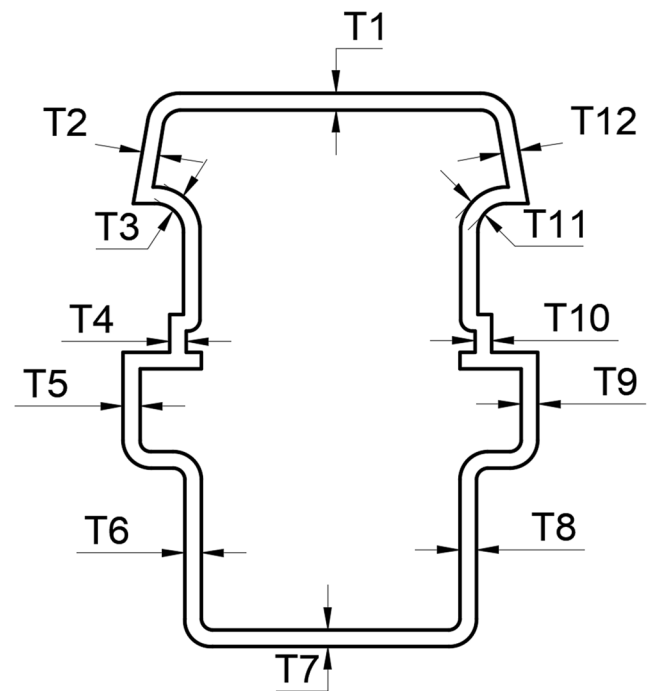


Fig. 12 Twelve position points in cross section of extruded parts

### 4 Conclusions

An improved inverse design method with CFD simulation shows advantages for thin-wall hollow profile extrusion die design. With complexity cross-section of a profile, the design can compensate the extrusion deformation and thickness change to get the right dimension of the product more effectively. It can be concluded:

- i. Simulation results show that the inlet flow rate and length of free jet should be appropriately chosen, which leads to proper thickness and geometry profile enlargement of the die lip gap.

Table 3 Measured value of 12 position points in cross-section of extruded parts

No.	Thickness (A) [mm]	Thickness (B) [mm]	Thickness (C) [mm]
T1	1.40	1.40	1.31
T2	1.48	1.48	1.50
T3	1.48	1.49	1.34
T4	1.51	1.59	1.54
T5	1.35	1.40	1.36
T6	1.35	1.39	1.35
T7	1.50	1.41	1.47
T8	1.47	1.38	1.38
T9	1.47	1.43	1.40
T10	1.59	1.66	1.65
T11	1.55	1.45	1.48
T12	1.32	1.31	1.35

- ii. By using design criteria of the inverse design method of extrusion die, the optimal solution of the extrusion die design can be found.

Compared to the flow balance method used widely at present, the inverse design method does not need sectional areas divided and the complicated optimization procedure. As a direct result, computational efficiency can be significantly improved. However, for the thin wall extrudate with significantly different thickness sections, the inverse design method needs to improve its efficiency. The best choice is to achieve flow balance firstly by using optimization design methods, and then employ the improved inverse design method to obtain the final design of extrusion die. It will improve the design accuracy and minimize the manufacture risks, which has been proved by this study.

**Funding information** This work is supported by Six Talent Peaks Project in Jiangsu Province (Grant No. RJFW-051) and National Natural Science Foundation of China (Grant No. 51605414).

## References

- Kostic MM, Reifschneider LG (2006) Design of extrusion dies. *Encycl Chem Process* 10:633–649
- Rauwendaal C (2014) *Polymer extrusion*. Carl Hanser Verlag GmbH Co KG
- Carneiro O (ed) (2012) *Design of extrusion forming tools*. Smithers Rapra
- Cho JR, Choi JH (2016) Numerical investigation of weather strip extrusion forming process by thermal flow analysis. *Int J Adv Manuf Technol* 87(9–12):2841–2851
- Fragassa C, Ippoliti M (2016) Technology assessment of tire mould cleaning systems and quality finishing. *Int J Qual Res* 10(3):523–546
- Mu Y, Hang L, Chen A, Zhao G, Xu D (2017) Influence of die geometric structure on flow balance in complex hollow plastic profile extrusion. *Int J Adv Manuf Technol* 91(1–4):1275–1287
- Tanner RI (1970) A theory of die-swell. *J Polym Sci A* 8:2067–2078
- Li L, Tang H, Guo S, Huang L, Xu Y (2017) Design and implementation of an integral design CAD system for plastic profile extrusion die. *Int J Adv Manuf Technol* 89(1):543–559
- Carneiro OS, Nobrega JM (2004) Recent developments in automatic die design for profile extrusion. *Plast Rubber Compos* 33(9–10):400–408
- Pittman JFT (2011) Computer-aided design and optimization of profile extrusion dies for thermoplastics and rubber: a review. *Proc Inst Mech Eng E J Process Mech Eng* 225(4):280–321
- Gonçalves ND, Teixeira P, Ferrás LL, Afonso AM, Nóbrega JM, Carneiro OS (2015) Design and optimization of an extrusion die for the production of wood–plastic composite profiles. *Polym Eng Sci* 55(8):1849–1855
- Gonçalves ND, Pereira SP, Ferrás LL, Nóbrega JM, Carneiro OS (2015) Using the GPU to design complex profile extrusion dies. *Int Polym Process* 30(4):442–450
- Zhang C, Chen H, Zhao G, Zhang L, Lou S (2016) Optimization of porthole extrusion dies with the developed algorithm based on finite volume method. *Int J Adv Manuf Technol* 85(5–8):1901
- Szarvasy I, Sienz J, Pittman JFT, Hinton E (2000) Computer aided optimisation of profile extrusion dies: definition and assessment of the objective function. *Int Polym Process* 15(1):28–39
- Carneiro OS, Nóbrega JM, Pinho FT, Oliveira PJ (2001) Computer aided rheological design of extrusion dies for profiles. *J Mater Process Technol* 114(1):75–86
- Zhang C, Yang S, Zhang Q, Zhao G, Lu P, Sun W (2017) Automatic optimization design of a feeder extrusion die with response surface methodology and mesh deformation technique. *Int J Adv Manuf Technol* 91:3181
- Pauli L, Behr M, Elgeti S (2013) Towards shape optimization of profile extrusion dies with respect to homogeneous die swell. *J Non-Newtonian Fluid Mech* 200:79–87
- Siegbert R, Behr M, Elgeti S (2016) Die swell as an objective in the design of polymer extrusion dies. In *AIP Conference Proceedings* (Vol. 1769, no. 1, p. 140003). AIP Publishing
- Siegbert R, Yesildag N, Frings M, Schmidt F, Elgeti S, Sauerland H, Vroomen U (2015) Individualized production in die-based manufacturing processes using numerical optimization. *Int J Adv Manuf Technol* 80(5–8):851–858
- Yilmaz O, Gunes H, Kirkkopru K (2014) Optimization of a profile extrusion die for flow balance. *Fibers Polym* 15(4):753–761
- Carneiro OS, Rajkumar A, Ferrás LL, Fernandes C, Sacramento A, Nóbrega JM (2017) Computer aided die design: a new open-source methodology. In *AIP Conference Proceedings* (Vol. 1843, no. 1, p. 030008). AIP Publishing
- Rajkumar A, Ferrás LL, Fernandes C, Carneiro OS, Becker M, Nóbrega JM (2017) Design guidelines to balance the flow distribution in complex profile extrusion dies. *Int Polym Process* 32(1):58–71
- Covas JA, Carneiro OS, Brito AM (1991) Designing extrusion dies for thermoplastics. *J Elastomers Plast* 23(3):218–238
- Legat V, Marchal JM (1993) Die design: an implicit formulation for the inverse problem. *Int J Numer Methods Fluids* 16(1):29–42
- Gifford WA (2003) Compensating for die swell in the design of profile dies. *Polym Eng Sci* 43(10):1657–1665
- Ordieres J, López LM, Bello A, Garcia A (2003) Intelligent methods helping the design of a manufacturing system for die extrusion rubbers. *Int J Comput Integr Manuf* 16(3):173–180
- Urraca R, Pernía-Espinoza A, Díaz I, Sanz-García A (2017) Practical methodology for validating constitutive models for the simulation of rubber compounds in extrusion processes. *Int J Adv Manuf Technol* 90(5–8):2377
- CAMPUS 5.2. <http://www.campusplastics.com>, Computer aided material preselection by uniform standards. Accessed 26 June 2018
- Nóbrega JM, Carneiro OS, Oliveira PJ, Pinho FT (2003) Flow balancing in extrusion dies for thermoplastic profiles: part I: automatic design. *Int Polym Process* 18(3):298–306
- Dai YK, Zhou CX, Yu W (2007) Inverse designing simulation of extrusion die of auto rubber seal and verifications. *Plast Rubber Compos* 36(4):141–148
- Legat V, Marchal JM (1992) Prediction of three-dimensional general shape extrudates by an implicit iterative scheme. *Int J Numer Methods Fluids* 14(5):609–625
- Goublomme A, Draily B, Crochet MJ (1992) Numerical prediction of extrudate swell of a high-density polyethylene. *J Non-Newtonian Fluid Mech* 44:171–195
- Ajiboye JS, Adegemi MB (2007) Upper bound analysis for extrusion at various die land lengths and shaped profiles. *Int J Mech Sci* 49(3):335–351

**Publisher's note** Springer Nature remains neutral with regard to jurisdictional claims in published maps and institutional affiliations.